

# Lithographic aspects for the fabrication of BiCMOS embedded Bio-MEMS and RF-MEMS

**P. Kulse, M. Birkholz, K.-E. Ehwald, M. Kaynak, M. Wietstruck,  
J. Bauer, J. Drews, K. Schulz**

IHP, Im Technologiepark 25, D-15236 Frankfurt (Oder), Germany, [kulse@ihp-microelectronics.com](mailto:kulse@ihp-microelectronics.com)

## ABSTRACT

Latest developments in micro-electro-mechanical systems (MEMS) have paved the way to follow the more than Moore approach. Several key components, such as silicon pressure sensors have been developed using MEMS processing techniques. Recently, MEMS technologies have been combined with standard CMOS processes and MEMS devices such as microviscosimeters and RF-MEMS switches were successfully demonstrated. The most challenging part of this MEMS process is the last long wet etch step, which remove the sacrificial layer to make the actuator moveable. Such long etch step is strongly influenced by the previous lithography steps. Especially the type of the photoresist has a strong influence on the performance of the final MEMS device. Here, we report a novel MEMS fabrication process, applied to the back-end-off-line (BEOL) of a 0.25 $\mu\text{m}$  SiGe BiCMOS technology. The full MEMS process flow is explained and the last lithography step is detailed. First, we show the influence of different substrate surface preconditions which defines the adhesion between the photoresist and the substrate. The final 6 $\mu\text{m}$  thick photoresist layer is required for the critical MEMS actuator release procedure due to the long wet etch process. In this wet etch process, a buffered hydrofluoric acid etchant penetrates the resist layer due to the long etch time (>80 min). Such penetration becomes more critical in the case of low adhesion between the photoresist and the wafer surface. Improving the latter can be achieved by using different primers or dehydration bakes. Furthermore, a new approach of an alternative standard lithography process is investigated. For both studies, additional SEM cross sections and contact angle measurements is presented.

**Key Words:** MEMS, Bio-MEMS, RF-MEMS, Surface promoter, HMDS

## 1. INTRODUCTION

Embedded micro-electromechanical systems (MEMS) continuously expand their key role for low energy consumption and highly reliable multi-sensor applications. Various MEMS devices have been developed so far, with actuators fabricated in bulk silicon like pressure sensors [1] or RF switches [2]. Indeed, recent developments make usage of elastically bendable structures with minimum feature dimensions in the micrometer and nanometer range from the back end of line (BEOL) of a standard 0.25 $\mu\text{m}$  BiCMOS technology as seen in [3]. In addition to embedded RF-MEMS switches [4], already established in microelectronic applications, Bio-MEMS provide a high potential for applications in different fields of healthcare. In here, we propose a promising approach by embedding a microviscosimeter [5] for continuous glucose monitoring in diabetic patients.

Hereby the subsequently processed BEOL module, used to realize the Bio-MEMS, comprises four metal layers (M1-M4), whereby each layer consists of a Ti/TiN/AlCu/Ti/TiN metal stack. For the purpose of TiN MEMS fabrication [6], a few changes of the standard flow of the BEOL module are necessary, as described in the following. A first modification of the standard flow is introduced after the M3 metal layer deposition and structuring. Consecutively, the top TiN/Ti and AlCu layers are removed by dry etching and a subsequent wet etch process, where the thin 50nm bottom TiN layer, used for the later MEMS structures, is not attacked due to the high selectivity of the etchant (Fig.1a-c). Then the standard preparation continues up to the chemical vapor deposition of the passivation layer and the bond pad openings. The schematic in Fig. 1d illustrates the BEOL architecture at this point of the process. In the next step (Fig. 1e) the passivation stack consisting of 390nm SiO<sub>x</sub>N<sub>y</sub> and 1250nm SiO<sub>2</sub> is partially etched in the area around the actuator by a

time-controlled reactive ion etch (RIE) step. The  $\text{SiO}_x\text{N}_y$  layer has to be removed due to the etch rate difference to  $\text{SiO}_2$  in the last wet etch process as illustrated in Fig. 1e.

In the following procedure all polymer residuals are removed and a surface preconditioning for the last lithography process step is performed with a forming gas treatment (FGT) at  $420^\circ\text{C}$  for 30min. This is used to dehydrate the whole wafer surface in order to increase the adhesion of the special HF wet etch-resistant novolak resist (ARP3100, Allresist), which is used in the last critical lithography step (Fig. 1f). The film thickness for this process is set to  $6\mu\text{m}$ . In addition to the forming gas treatment, a liquid Ti primer (TI Prime, MircoChemicals) is used for enhancing the resist adhesion to the substrate. The following i-line exposure ensures the complete opening of windows with dimensions of  $145\mu\text{m} \times 57\mu\text{m}$  without any resist residuals (Fig. 2) by applying a high exposure dose of 1800ms in total. Thereby the process is split into two exposing steps with 900ms to avoid bubbling of the resist during exposure.

Afterwards, the TiN actuators, which are situated in the M3 metal layer, are released from the surrounding  $\text{SiO}_2$  of the inter-layer dielectric (ILD). A special hydrofluoric containing etching solution removes the  $\text{SiO}_2$  of the inter-layer dielectric with a high selectivity to TiN from the M1 ground plate. Here, the top Ti/TiN metal layer of the M1 ground plate acts as an intrinsic etch stop layer. In addition, this etch procedure also completely removes the Ti layer situated underneath the TiN actuator beam. During the long wet etch process ( $>80$  min) the buffered hydrofluoric acid etchant penetrates the resist layer. Such penetration becomes more critical in the case of low adhesion between the resist and the wafer surface which leads to large scaling under etch of the  $\text{SiO}_2/\text{SiO}_x\text{N}_y$  passivation layer or even etching the adjacent AlCu layer of the TiN actuator (Fig. 3).

The already established special MEMS lithography successfully ensures a MEMS actuator releasing procedure without these effects. Nevertheless, the special MEMS lithography process suffers from a low throughput and high cost level by the exclusive usage of the Ti Primer and special ARP3100 resist in the whole technology flow. In addition, degassing resist solvents increase the risk of contamination of the final optical element during the exposing procedure, cause of the  $6\mu\text{m}$  resist film thickness (FT) which require to apply a double high exposure dose job with 900 ms.

Here, we presented a solution to transfer the special MEMS lithography to a more compatible litho process for a standard  $0.25\mu\text{m}$  BiCMOS technology. Therefore we identify a  $\text{SiO}_2$  wet etch resistant ( $t_{\text{etch}} > 80\text{min}$ ) resist and demonstrate by enhancing the substrate surface hydrophobicity the usability of a lower resist FT to realize a lower exposure dose.

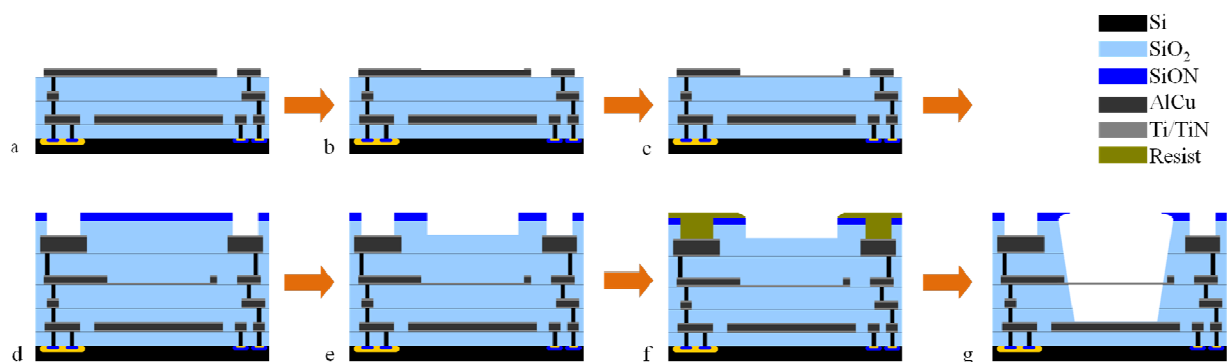


**Fig. 1.** Fabrication sequence for the TiN actuators from the metal 3 layer from the IHP's  $0.25\mu\text{m}$  BiCMOS technology. Detailed description for the process steps: a) Structuring of full metal 3 stack b) Dry etching of top TiN layer c) Wet etching of metal 3 AlCu d) Metal 4 Bond pad opening via dry etching e)  $\text{SiO}_x\text{N}_y$  removal above MEMS cavity f) Developed resist mask after special MEMS lithography process g) Released TiN actuator after long  $\text{SiO}_2$  wet etch process

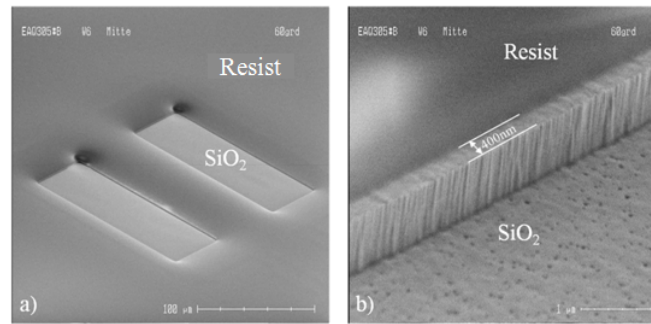


**Fig. 2.** Sub picture a illustrates the round shaped resist mask topology without remaining polymers and the hastate resist coating effect which results in the gap of 400nm between the resist mask and the step in the passivation layer b) formed by the previous dry RIE etch process.

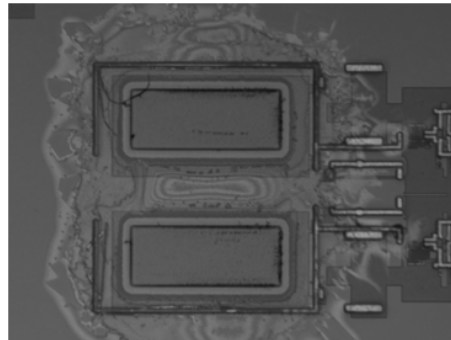


**Fig. 3.** Result of large scaling under etching behavior of the  $\text{SiO}_2/\text{SiO}_x\text{N}_y$  passivation layer due to a low adhesion between resist mask and substrate surface.

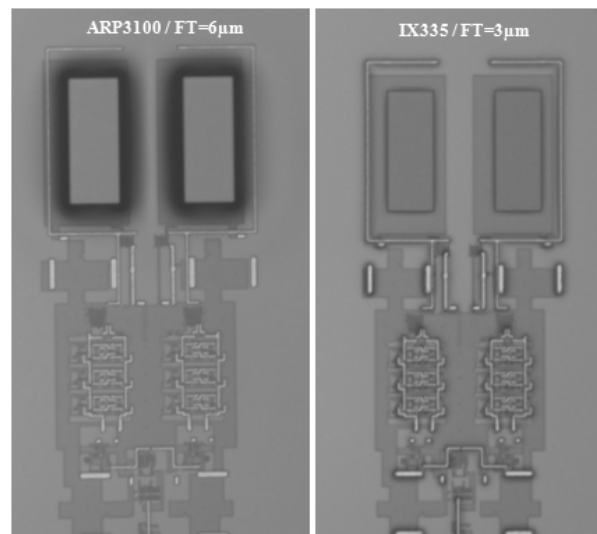
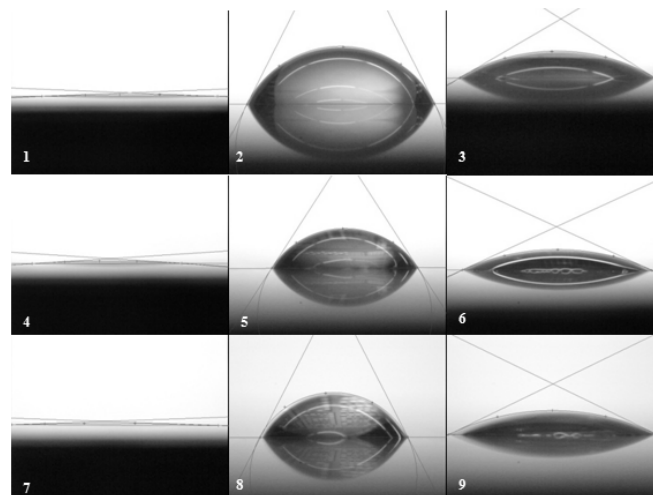
## 2. EXPERIMENTAL

For the initial experiments a short flow is prepared which only include the M1 and M4 metal layer and the corresponding  $\text{SiO}_2$  dielectric inlayers. Therefore, two types of positive tone resists in combination with different primers with and without the FGT process are used. The wet etch stable novolak resist ARP3100 with a viscosity of  $\eta=180\text{cp}$  and the IX335 (JSR Electronics) resist with a viscosity of  $\eta=60\text{cp}$  are used in this experiments. We use a FGT process whereby the whole wafer is heated up to  $420^\circ$  for 30min in a  $\text{NH}_3$  atmosphere. After tempering and therefore dehydrating the wafer surface the priming and coating follows subsequently. As a matter of fact that the liquid Ti Primer has to coat separately there has to be no lay time between the following resist coating step. Otherwise a decreasing resist adhesion can be observed. The hexamethyl disilazane (HMDS) adhesion promoter is applied by subjecting the substrate to HMDS vapor at  $120^\circ\text{C}$  for 30sec. This inline process can be applied directly before the coating process for both resists. Table 1 summarizes the different wafer preparations for the experiments. Besides table 1, figure 3 shows the different quality of the developed ARP3100 and IX335 resist masks due to the reduced FT and exposure dose for IX335. For the FGT experiments we introduced a general idle time or lay time of max. 3h to avoid a decreasing resist adhesion. All experiments are done with a Nikon i-line stepper NSR-2205 i-11D and DNS wafer track. Finally, all wafers are etched and SEM cross sections are performed. Based on these SEM cross sections the under etching of the resist mask are determined.

For the contact angle measurements (measurement device: SURFTENS from OEG GmbH) we use water ( $16\text{-}17\text{M}\Omega\text{cm}$ ) as test liquid. Maximum 3h after the FGT process the wafers are primed and the contact angle of a drop of water is measured three times on variable positions at the wafer surface. Also bare Si wafers and blank  $\text{SiO}_x\text{N}_y$  surfaces are measured for comparison with the primed surfaces. After applying the single water drops, pictures are taken and contact angles are determined as shown in Table 2.

**Table 1.** Experimental overview of different wafer preparation.

Wafer	Surface	FGT 420°C	Priming	Resist / FT	Exposure dose (ms)
10	SiO <sub>x</sub> N <sub>y</sub>	X	HMDS	ARP3100 / 6μm	2 x 900
11	SiO <sub>x</sub> N <sub>y</sub>	X	Ti Prime	ARP3100 / 6μm	2 x 900
12	SiO <sub>x</sub> N <sub>y</sub>	X	HMDS	IX335 / 3μm	500
13	SiO <sub>x</sub> N <sub>y</sub>	X	Ti Prime	IX335 / 3μm	500
14	SiO <sub>x</sub> N <sub>y</sub>		Ti Prime	ARP3100 / 6μm	2 x 900
15	SiO <sub>x</sub> N <sub>y</sub>		HMDS	ARP3100 / 6μm	2 x 900

**Fig. 4.** Microscopic topview of the Bio-MEMS integrated circuit without TiN MEMS actuator. Left figure shows the characteristic wide slope of the ARP3100 resist after development. The IX335 in contrast shows a fine sharp slope because of a lower FT.**Fig. 5.** The applied water drops in picture one to nine showing the different contact angles due to various substrate surface treatments as listed in table 2.

**Table 2:** Results from contact angle measurements of different surfaces and adhesion promoters. The determination is realized with the special software SURFTENS (OEG GmbH).

Wafer	Surface	FGT 420°C	Priming	Contact angle $\theta$
1	bare Si			2.26°
2	bare Si		HMDS	63.02°
3	bare Si		Ti Prime	33.88°
4	SiO <sub>x</sub> N <sub>y</sub>			3.72°
5	SiO <sub>x</sub> N <sub>y</sub>		HMDS	56.97°
6	SiO <sub>x</sub> N <sub>y</sub>		TI Prime	24.58°
7	SiO <sub>x</sub> N <sub>y</sub>	X		2.02°
8	SiO <sub>x</sub> N <sub>y</sub>	X	HMDS	62.68°
9	SiO <sub>x</sub> N <sub>y</sub>	X	Ti Prime	25.86°

### 3. RESULTS AND DISCUSSION

First results of the contact angle from bare Si wafer surfaces are shown in table 2. It can be clearly seen that the very low  $\theta$  of 2.26° on the blank Si surface indicates a super hydrophilic behavior. In contrast to the Ti Prime treated surface the HMDS coated surface shows the typically optimum  $\theta$  value for a good resist adhesion [7]. By focusing on the top layer of the SiO<sub>x</sub>N<sub>y</sub>/SiO<sub>2</sub> wafer passivation, a reduced  $\theta_{\text{HMDS}}$  and  $\theta_{\text{Ti Prime}}$  for the FGT untreated SiO<sub>x</sub>N<sub>y</sub> surface can be observed. Nevertheless, it is still obvious that the fact  $\theta_{\text{HMDS}} > \theta_{\text{Ti Prime}}$  indicates a slightly better resist adhesion during the development and wet etching process due to the higher hydrophobic surface.

In first experiments (table 1 wafer 14, 15) the established MEMS lithography process is investigated with both adhesion promoters but still with the special ARP3100 resist. Therefore, the results after the long wet etching mentioned in table 3 shows same under etching for the length and width of both resist mask and primers. Cause of the relative low  $\theta_{\text{Ti Prime}}$  one estimates a higher under etching compared to the HMDS treated surface. This impressive case demonstrates the specific chemical engineering of the ARP3100 resist in combination with the Ti Prime adhesion promoter for SiO<sub>2</sub> wet etch processes. However, this experiments and contact angle measurements points out the general usability of the HMDS primer for a long SiO<sub>2</sub> wet etch process.

In the following experiments from table 2 the impact of an additional included FGT process will be studied. Thereby, the contact angle measurements show a shifting  $\theta_{\text{HMDS}}$  value, whereas counter-intuitively the contact angle of the Ti Primer remains the same. Based on these results, wafer 11 and 13 from table 1 are etched and compared by the amount of resist mask under etching. The results underline the specific chemical engineering of the ARP3100 resist in combination with the Ti Prime adhesion promoter for SiO<sub>2</sub> wet etch process. Wafer 13 with the HMDS promoter produces the former described large scaling under etch effect illustrated in Fig. 2. Inversely, the under etching of the length and width on wafer 11 reduces about 9 $\mu\text{m}$  in each case determined by SEM cross sections (Fig. 6a) and microscopy pictures (Fig.6c) in comparison to wafer 14. Assuming that the additionally FGT process corresponds with an increase of  $\theta_{\text{Ti Prime}}$  by 1.28° results in a bilateral 9 $\mu\text{m}$  lower under etching, it seems to be obvious that the IX335 resist show the same behavior after the FGT process. In former studies the IX335 are investigated but without the FGT process and shows the above mentioned large scaling etching effect like the example in Fig.2.

On that account, wafers 10 and 12 were prepared, etched and the etch results determined by SEM cross sections. Wafer 10 with the ARP3100 resist and HMDS primer stays nearly the same length and width under etching results as wafer 11 before. Unexpectedly, the etch results for wafer 12 seen in SEM cross section (Fig. 6b) and microscopy picture (Fig. 6d) are the same as the best results with the ARP3100 resist and Ti Prime adhesion promoter from wafer 11. In both cases the layout length of 145 $\mu\text{m}$  and the width of 57 $\mu\text{m}$  are expand of about 16 $\mu\text{m}$  and 17 $\mu\text{m}$  at both sides.

Compare wafer 11 and 12 the resist FT with  $3\mu\text{m}$  of the IX335 is only the half of ARP3100 FT with  $6\mu\text{m}$  due to the one third viscosity ( $\eta_{\text{ARP3100}}=180\text{cp}$ ,  $\eta_{\text{IX335}}=60\text{cp}$ ). As a matter of fact that the exposure dose is directly linked to the resist FT it explains the much lower exposure dose of 500ms for the IX335. This prevents the resist of outgasing solvents and bubbling during the exposure, which can potentially increase the risk of contamination of the final optical element of the lithography exposure tool. Another beneficial result illustrates the SEM cross section of the IX335 (Fig. 6b) which shows still the same fine sharp slope after the development like in Fig. 4. These observations allow concluding that the IX335 shows the equal high etch resistivity as the ARP3100 for a  $\text{SiO}_2$  wet etch process. Finally, by including an FGT step it is possible to realize the special MEMS lithography procedure with more standard like lithography, which implies a lay time of max. 3h, a HMDS adhesion promoter and the IX335 resist.

For future work the dependency from various lay times between the FGT process and the priming and coating procedure have to be investigated in detail. Therefore further experiments have to be done to get a predication about the correlation between laytime and resist adhesion otherwise the lay time can be a potential throughput restrictor. Another issue which limits the usage of the IX335 resist is the maximum FT of  $3\mu\text{m}$ . If a topology of more than  $3\mu\text{m}$  below the resist layer exists resist ablation and inhomogeneous resist distribution and leads to huge under etching. One possible solution for this scenario is an application of other novolak resists or applying the IX335 in another dilution to achieve a FT of  $6\mu\text{m}$ . Indeed, in case of other novolak resists the experiments has to be repeated cause of the certainly quite different reaction in a long wet etch process.

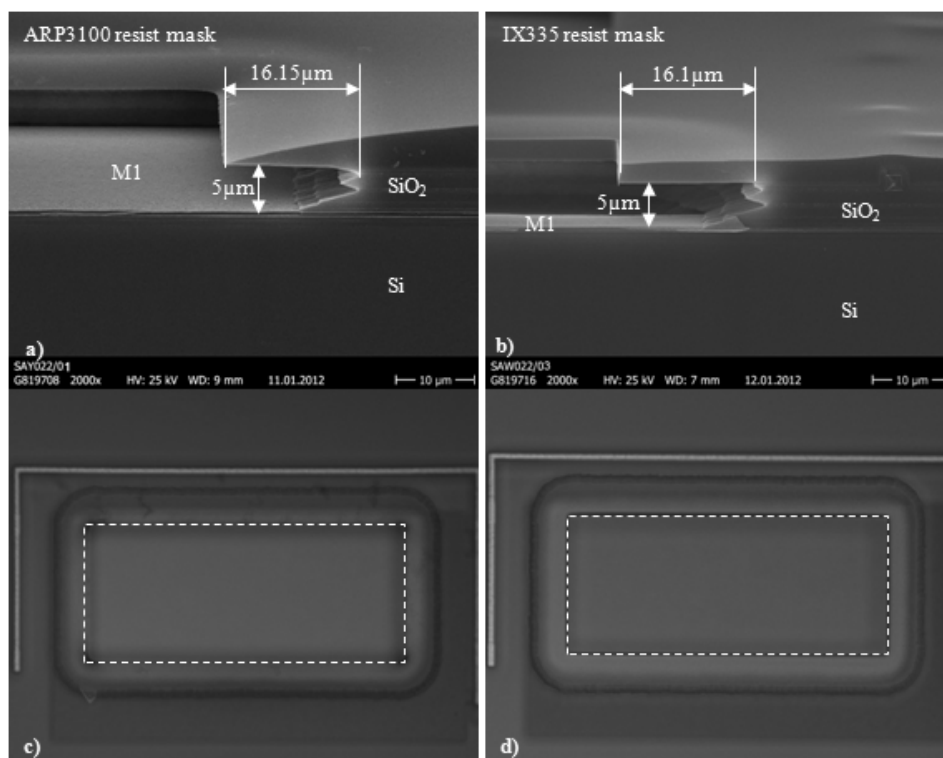


**Fig. 6.** Sub picture a) illustrates the round shaped resist profile of the ARP3100 resist above the under etched  $\text{SiO}_2$  layers. The dashed line in c) shows the front tip of the resist profile seen in a). Furthermore, the under etched areas can be clearly seen in c) around the dashed line. In comparison to the ARP3100 resist profile the IX335 resist demonstrate the typical bride edge illustrated in b). Like the ARP3100 the IX335 has the same amount of under etched  $\text{SiO}_2$  layers which is pointed out in d). There the surrounding gap between the dashed line and the under etched region in d) looks the same as c).

**Table 2:** Experimental results of the measured under etching for one side in length and width after the long SiO<sub>2</sub> wet etch process. The total under etching amount can be determined by  $\text{Etch}_{\text{Under}} = l_{\text{Layout}} + 2x (l_{\text{measured}})$

Wafer	Under etching	
	Layout $l = 145\mu\text{m}$ $w = 57\mu\text{m}$ measured length and width	
	length $\mu\text{m}$	width $\mu\text{m}$
10	16.65	17.3
11	16.15	16.7
12	16.1	16.5
13	-	-
14	20.75	21
15	20.8	21.25

#### 4. CONCLUSION

In this contribution we demonstrate how an additional forming gas temper process step improved the contact angle and therefore the resist adhesion for a HMDS coated SiO<sub>x</sub>N<sub>y</sub> surface and reduces the under etching during a long wet etch process (>80min). We determine a maximum idle period of 3h between the FGT and coating procedures to ensure sufficient resist adhesion to the SiO<sub>x</sub>N<sub>y</sub> surface. First we show a special MEMS lithography process and additionally describe an alternative more standard like lithography process. Here, both types of wet etch stable novolak resists showing the same wet etching resistivity in the long SiO<sub>2</sub> wet etch process. Furthermore, we successfully introduce an enhanced more standard like MEMS lithography process into the IHP 0.25 $\mu\text{m}$  BiCMOS technology. Finally, an optimization of the process throughput and costs by saving the Ti Prime adhesion promoter and ARP3100 resist are realized.

#### References

- [1] S. Chu, S.K. Gamage, H-J. Kwon, US Patent No. 7,622,782 B2.
- [2] J-M. Kim, S. Lee, J-H. Park, C-W. Baek, Y. Kwon, Y-K. Kim, J. Micromech. Microeng. **20** (2010) 095007.
- [3] D. Knoll et al., IEDM Technical Digest (2002) 783.
- [4] M. Kaynak et al., IEDM Technical Digest (2009) 787
- [5] M. Birkholz et al., Mikrosystemtechnik Kongress 2009, Berlin, (2009), 124.
- [6] M. Birkholz et al., Advanced Functional Materials **21** (2011) 1652.
- [7] Levinson, H.J., 2005, Principles of Lithography, second edition, SPIE Press (Bellingham, WA), p. 59